

# A Study of the Chemical and Physical Mechanisms of Fire Suppression by Water

ARVIND ATREYA, TODD CROMPTON and JAEIL SUH  
Department of Mechanical Engineering and Applied Mechanics  
The University of Michigan  
Ann Arbor, MI 48105

## ABSTRACT

This work attempts to develop a quantitative understanding of the chemical and physical gas-phase fire suppression mechanisms of water. Small-scale diffusion flame experiments and calculations with detailed kinetics are done to study these gas-phase effects. The experimental results show that there is a significant chemical enhancement effect due to increased water vapor concentration in the flame zone. This effect reduces the soot concentration and oxidizes CO to CO<sub>2</sub>. Consequently, the combustion becomes more complete and the flame temperature is increased as the water concentration is increased. The actual magnitude of the chemical enhancement, however, depends on the water concentration, the O<sub>2</sub> concentration and the flame temperature. Mixing caused by liquid water application and water evaporation may significantly affect the gas composition. In particular, it may increase the CO concentration for a low O<sub>2</sub> concentration fire environment. It was also found that an increase in the water vapor concentration considerably enhances the radiative heat loss from the flame. This heat loss becomes less significant with increase in the strain rate due to a reduction in the flame zone thickness.

**KEYWORDS:** Fire suppression, water, chemical enhancement, diffusion flames, flame temperature, flame radiation, strain rate.

## INTRODUCTION

An understanding of the effect of water on fire is of considerable interest due to its widespread use in fire suppression. Water is and will continue to be a premier suppression agent because it is non-toxic, abundant and inexpensive. Health and environmental concerns limit the use of other chemical agents such as halons and dry chemical powders. However, there is a lack of quantitative information on fire suppression by water. In the words of Rasbash [1], a pioneer in the field, "It is probably safe to say that since mankind first made use of fire, they made use

of water to control it. Apart from rhetorical quotations, very little has come down to us from aeons of time, on just how much water is needed to control fires of different kind." Later in the review article, Rasbash recommends "...more experimental work aimed at improving our understanding of the phenomena involved ...". This study is an attempt to provide some understanding regarding the fire suppression mechanisms of water by the use of small-scale experiments and models.

Previous literature [1-6, and references therein] shows that water has two physical effects: (i) cooling of the burning solid by water evaporation, and (ii) smothering caused by dilution of the oxidizer and/or the fuel by water vapor. In addition to these two well-known effects, there are three more effects, namely: (iii) enhanced radiative heat loss due to increased water concentration, (iv) enhanced mixing as a result of volumetric expansion caused by water evaporation, and (v) a little known but significant chemical enhancement effect which reduces the soot concentration and decreases the luminous flame radiation.

Water is typically sprayed as a liquid onto the fire. However, usually excessive amounts of water is used which often causes as much or more property damage as the fire. Liquid water sprays are also not suitable for electronic items, liquid fuel fires, and certain metals and chemicals. Thus, while cooling of the burning condensed phase by water evaporation is the most effective suppression mechanism of water, it appears that for reduction in property damage and for wider application, we must rely only on its gas-phase suppression mechanisms. This realization has led to the use of water mist which has fine droplets that do not directly reach the burning object but instead cool and dilute the surrounding gases. Water mist is also being considered as a possible replacement of halons [7]. Since the physical cooling effect of water (i.e., (i)) has been studied earlier [8,9], developing a fundamental understanding of the gas-phase suppression mechanisms of water (i.e., (ii) through (v)) will be very helpful.

Unfortunately, little is known about the effects (iv) and (v). Previous work on premixed flames [10,11] shows that the burning velocity is significantly affected by the presence of steam. It was concluded that water is not just inert, instead it chemically interacts in the flame. In sooting diffusion flames, that are more representative of a fire, it was found [12] that water is much more effective than  $\text{CO}_2$  at reducing the sooting tendency possibly because of increased production of OH by water vapor. Yet, other researchers [13,14] find the effect of water to be purely thermal (i.e. due to heat capacity). The experiments described here attempt to resolve this controversy and quantify the increase in the combustion efficiency and the resulting reduction in the suppression effectiveness of water (defined as the decrease in the heat release rate per unit mass application rate of the suppression agent).

To quantify these gas-phase effects of water, small-scale experiments on radiative counterflow diffusion flames are conducted. These are chosen because they represent the local behavior of buoyant turbulent diffusion flames (fires) and are convenient for both experimental measurements and theoretical modeling. Transient experimental results of the effect of water are first presented, followed by calculations of the flame structure to investigate the effect of flame radiative heat loss.

## EXPERIMENTAL APPARATUS

A unique closed axis-symmetric stagnation-point-flow flame apparatus was designed to study

the suppression mechanisms. It is schematically shown in fig.1. A detailed description of this apparatus and the calibration procedure is presented elsewhere [15]. This apparatus is designed for conducting small-scale transient suppression experiments with a liquid or a vapor agent. The agent may be applied to a steadily burning solid in the stagnation-point-flow configuration or to a counterflow diffusion flame formed by a porous ceramic gas burner which replaces the 38.1mm diameter fuel specimen. The oxidizer enters the upper temperature-controlled cylindrical heaters with a center ceramic tube for gas supply. This ceramic tube supports a ceramic honeycomb heat exchanger and flow straightener. The final oxidizer exit is 63.5mm in diameter. The cylindrical heaters are supported by a specially designed ceramic flange which is supported by a water-cooled stainless-steel cylinder. An outer concentric stainless-steel casing is used to direct the exhaust gases through the annular opening. A 305mm diameter quartz cylinder that can slide over the stainless-steel casing is used as an observation window. It is sealed to prevent gas leakage. The test sample is surrounded by ceramic insulation to ensure one-dimensional heat conduction. A water-cooled droplet tube that can swing in and out of the hot burner zone is used to release water droplets on the sample surface. Water in the vapor form is applied by simply adding it to the oxidizer or the fuel stream.

This apparatus permits the control of composition, temperature and velocity of the fuel & oxidizer streams. Most importantly, it permits transient measurements of the exhaust gas composition which enables quantifying the effect of the suppression agent and determine the suppression rate (defined as the attenuation in the heat release rate). Continuous gas analyzers were used for measuring  $H_2O$ ,  $CO_2$ ,  $CO$  and  $O_2$  in the exhaust. The gas concentration measurements, reported here, were corrected for the transport time and the detector response time [16]. Calibration experiments were done to show that suppression transients of order '1 sec' can be resolved and that the overall mass balance was within 5%. In addition, temperature measurements across the one-dimensional diffusion flame were made by coated *Pt/Pt-Rh* thermocouples and a video camera was used to continuously record the extinguishment history. These measurements in conjunction with an appropriate model are used to identify the suppression mechanisms and determine the chemical heat release rate.

**EXPERIMENTAL RESULTS**

**Suppression Experiments with Liquid Water**

Initial experiments were conducted with measured amounts of liquid water applied to the center of a steadily burning PMMA sample in the stagnation-point-flow configuration. The objective was to quantify the suppression rate. These experiments, while not reported here, produced

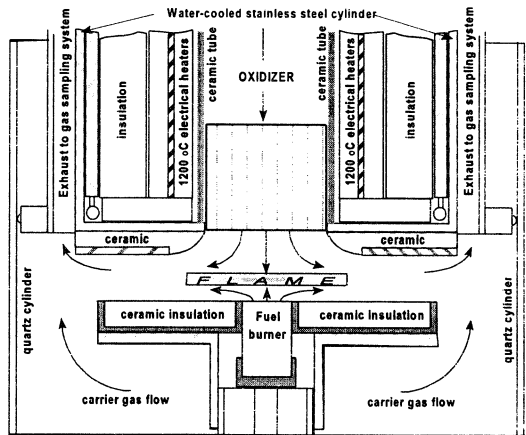


**FIGURE 1:** Cross-section of the closed axis-symmetric stagnation-point-flow suppression apparatus.

unexpected but interesting results. Measurements, that were checked numerous times for error, showed a considerable initial increase in the burning rate (as measured by  $CO_2$  production rate and  $O_2$  depletion rate) and a subsequent decrease due to physical cooling after the water had evaporated. Eventually, the solid recovered to its steady burning condition. This enhancement of the burning rate was only observed for sooty flames. To separate the chemical and physical effects of water, PMMA was replaced by a porous ceramic gas burner. Thus, physical cooling effect was eliminated leaving only dilution and chemical enhancement effects.

Methane was chosen as the fuel for the porous ceramic burner. The methane and oxidizer flow rates (1.5 & 10.5 lpm respectively) and the external radiation from the heaters ( $0.43 \text{ W/cm}^2$ ) were held constant during all the experiments conducted with different  $O_2$  concentrations (to change the sootiness of the flame) and different constant water application rates. Water was applied by a syringe pump through a small water-cooled stainless steel tube to the center of the porous ceramic burner. Transient species composition measurements in the exhaust were used to determine the effect of water droplets on the overall heat release rate. An increase in the  $CO_2$  production rate and  $O_2$  depletion rate corresponds to an increase in the burning rate and vice versa. Representative results for three different oxygen concentrations are presented here: (i) 12%  $O_2$  which produced a blue flame, (ii) 15%  $O_2$  which produced a sooty yellow flame, and (iii) 30%  $O_2$  which produced a high temperature bright sooty flame. Note that the incoming air stream was preheated by the heaters to 723K. This enabled low  $O_2\%$  flames to exist.

Blue  $CH_4$  flame (12%  $O_2$ ): Experimental results for a blue methane flame are presented in figures 2a-2c. These are corrected (for response time and transport time) gas concentration measurements in the exhaust as a function of time during which liquid water was applied on the porous ceramic burner (i.e. on the fuel side of the diffusion flame). Only  $CO_2$ ,  $CO$  and  $THC$  (total hydrocarbons) are presented here because the  $O_2$  depletion data is similar to the  $CO_2$  production data. Also, as can be seen from the high  $CO$  and  $THC$  concentrations prior to water application, the flame was blue and "weak" because insufficient  $O_2$  was available to burn all of the fuel supplied. These figures show that water application (during 300 to 1200sec) essentially diluted the fuel resulting in more incomplete combustion. The unburned hydrocarbon concentration increased and the  $CO_2$  concentration decreased as the water application rate was increased. At 13.3mg/sec water application rate the flame was extinguished. There is no evidence of chemical enhancement of the burning rate despite the presence of significant amounts of unburned hydrocarbons. This may be because the flame temperature was too low and water simply behaved as an inert diluent under these conditions. These results are in agreement with those reported by references [13, 14].

Sooty  $CH_4$  flame (15%  $O_2$ ): Results for a sooty methane flame are shown in figures 2d-3c. Here, except for the  $O_2\%$ , all other conditions were same as the blue flame. Increased oxygen concentration resulted in an increase in the flame temperature and the soot formation rate. Consequently, the flame was yellow. It is interesting to note that the  $CO_2$  production rate (Fig. 2d) first increased with the water application rate, then stopped increasing between 5.58 & 9.23mg/sec, and eventually decreased at 13.3mg/sec water application rate. Thus, if the  $CO_2$  production rate is taken as the exclusive measure of the suppression rate, the burning rate initially increased (due to chemical enhancement) and later decreased (due to dilution). However, if the  $O_2$  depletion rate (Fig. 3a) is simultaneously considered, the burning rate increased for all cases but the increase was less for the 13.3mg/sec water application rate. Clearly, there are two competing mechanisms: (i) chemical enhancement, and (ii) physical

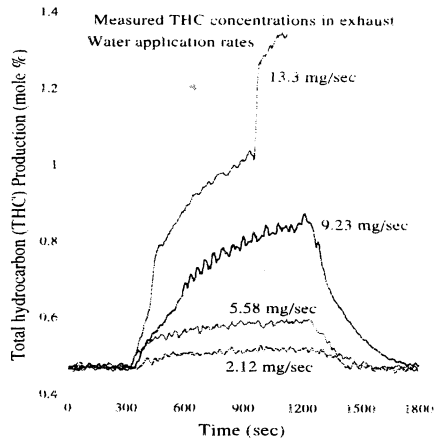
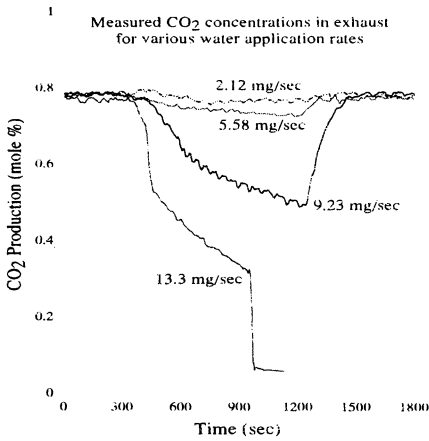


**Fig. 2a:** CO<sub>2</sub> for blue CH<sub>4</sub> flame at 12% O<sub>2</sub>. **Fig. 2b:** THC for blue CH<sub>4</sub> flame at 12% O<sub>2</sub>.

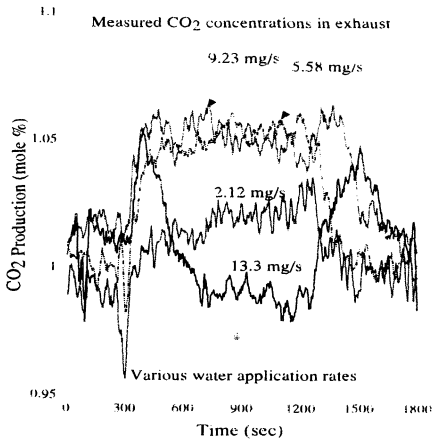
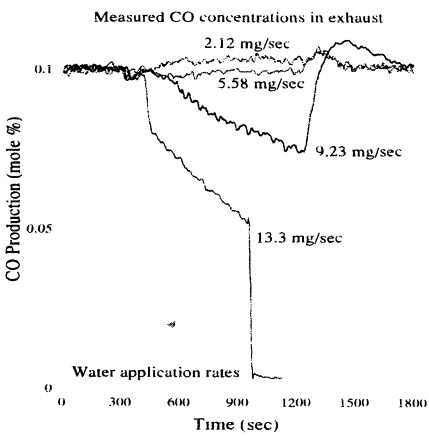


**Fig. 2c:** CO for blue CH<sub>4</sub> flame at 12% O<sub>2</sub>. **Fig. 2d:** CO<sub>2</sub> for sooty CH<sub>4</sub> flame at 15% O<sub>2</sub>

**FIGURE 2:** Species production rates during various liquid water application rates for blue and sooty CH<sub>4</sub> flames at 12% and 15% O<sub>2</sub> concentration in the hot (723K) oxidizer flow. Water application on the porous ceramic burner began at 300 sec and was stopped at 1200 sec.

dilution. Yet, it is curious how O<sub>2</sub> was consumed without producing CO<sub>2</sub>. The answer to this is clear from the CO production rates presented in figure 3b. Note that the CO production rate increased for all cases of the yellow flame, whereas it decreased for all cases of the blue flame. Due to insufficient oxygen, substantial amounts of CO along with CO<sub>2</sub> was produced. It also appears that the reduction in temperatures due to water application did not permit the water-gas reaction ( $CO + H_2O = CO_2 + H_2$ ) to equilibrate because it will tend to reduce CO as H<sub>2</sub>O% is increased. Finally, the total unburned hydrocarbons (Fig. 3c) always increased with increase

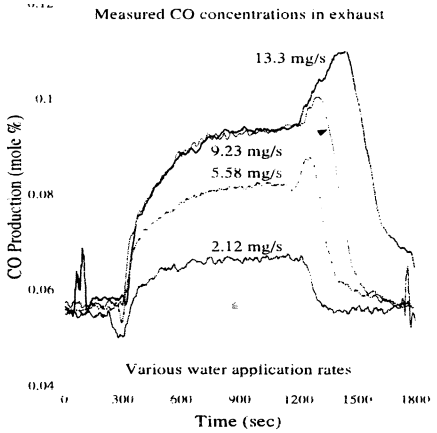
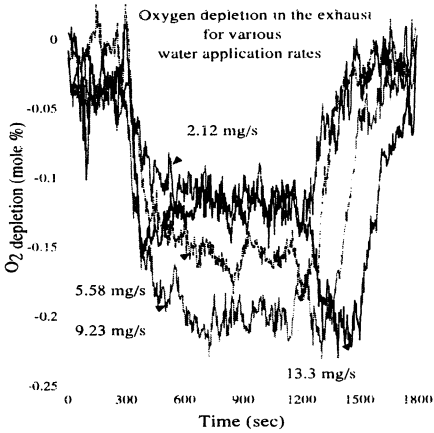


**Fig. 3a:**  $O_2$  for sooty  $CH_4$  flame at 15%  $O_2$ . **Fig. 3b:** CO for sooty  $CH_4$  flame at 15%  $O_2$ .

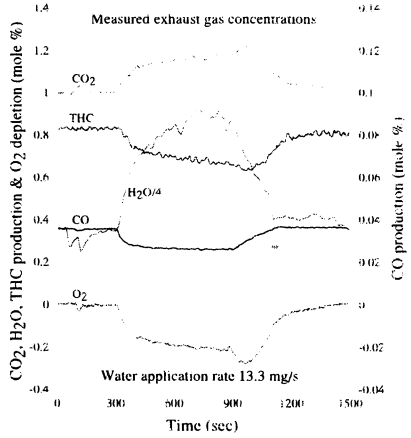
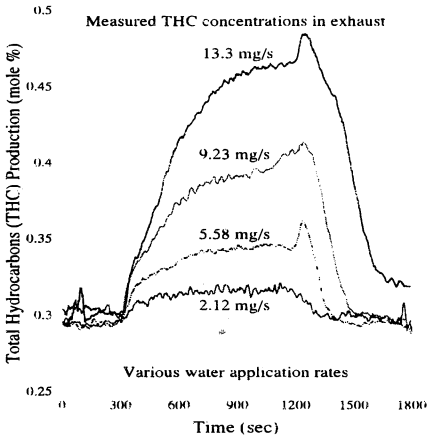


**Fig. 3c:** THC for sooty  $CH_4$  flame at 15%  $O_2$ . **Fig. 3d:** Species - sooty  $CH_4$  flame at 30%  $O_2$

**FIGURE 3:** Species production rates during various liquid water application rates for sooty  $CH_4$  flames at 15% and 30%  $O_2$  concentration in the hot (723K) oxidizer flow. Water application on the porous ceramic burner began at 300 sec and was stopped at 1200 sec.

in the water application rate. This implies lower fuel oxidation which is inconsistent with the increase in  $CO$  &  $CO_2$  production. This inconsistency is explained by noting that the soot production rate was substantially reduced (visual observations) and that the magnitude of total unburned hydrocarbons is significantly lower than that for the blue flame. Recall that the methane flow rate was held constant for all flames. Thus, water application reduced the soot formation rate perhaps by intervening in the soot inception process [12]. Some of the unburned hydrocarbons were oxidized to  $CO$  &  $CO_2$  while the rest escaped the flame. Note that this is

a reasonably realistic fire scenario because 15%  $O_2$  and fuel-rich conditions are not uncommon in a fire. These experiments point to a disturbing situation where the  $CO$  production rate may be increased by water suppression efforts.

**Bright sooty flame (30%  $O_2$ ):** Further increase in  $O_2\%$  makes the flame very bright yellow and sooty. Also, for the same flow rates of fuel and oxidizer, the flame moves closer to the porous ceramic burner surface. Since the flame temperature is significantly increased, water may become more chemically active in the flame. Typical results from only one of the several experiments conducted are presented in figure 3d. This figure is for 13.3mg/sec water application rate. Note that both  $CO$  and unburned hydrocarbons are oxidized to  $CO_2$  due to sufficient available  $O_2$ . Also, higher flame temperatures may enable the water-gas reaction to approach equilibrium. This will reduce  $CO\%$  as  $H_2O\%$  is increased

The above results clearly show chemical enhancement of the burning rate due to water application. Since these results contradict some previous work [13, 14] which claims that water simply acts as a diluent, the experiments were repeated with water vapor instead of liquid water. This was done to eliminate the possibility of enhanced mixing and flow disruptions that may have been caused by evaporation and the resulting volumetric expansion of liquid water. While this is possible and certainly occurs during actual fire suppression efforts, it was not visibly observed during these experiments.

### Suppression Experiments with Water Vapor

In the experimental results presented here, different amounts of water vapor was added to the oxidizer side flow. The flow rate of fuel with diluent (nitrogen) was 2 liter-per-minute, while that of the oxidizer with two different diluents (nitrogen and argon) was 8 liter-per-minute. These flow rates were held constant for all the experiments. While the experiments were conducted for  $CH_4$  and  $C_2H_4$  at 15%, 20% & 25%  $O_2$  [15], the results of only  $CH_4$  at 20%  $O_2$  are presented here. The input concentrations of fuel side flow were 75%  $CH_4$  and 25%  $N_2$  for all the flames. However, different amounts of water was substituted in the oxidizer flow and the resulting concentrations are summarized in Table 1.

The input composition of the oxidizer side flow was changed as a mixture of water-vapor and  $Ar$  was substituted for  $N_2$ . However, the oxygen concentration was not changed. A mixture of  $H_2O$  and  $Ar$  was substituted for  $N_2$  to keep the ' $\rho C_p$ ' product of the oxidizer flow constant while increasing the water concentration. The objective was to quantify the chemical effect of water without changing the primary

TABLE 1: Inlet conditions for the oxidizer flow

	(1)	(2)	(3)	(4)	(5)
$H_2O$	0%	10%	20%	30%	40%
$O_2$	20%	20%	20%	20%	20%
$N_2$	80%	61.6%	43.1%	24.7%	6.3%
$Ar$	0.0%	8.4%	16.9%	25.3%	33.7%

physical properties, i.e. dilution, density, strain rate and heat capacity. These experiments were performed using the following procedure. First, a steady diffusion flame was established with only  $N_2$  in the oxidizer stream (0% water) and the steady species concentrations were measured for 5 minutes. Then, the oxidizer stream concentrations were changed to the desired water concentration. This water flame was maintained for 15 minutes until steady conditions were established. Continuous species measurements were made throughout. Flame

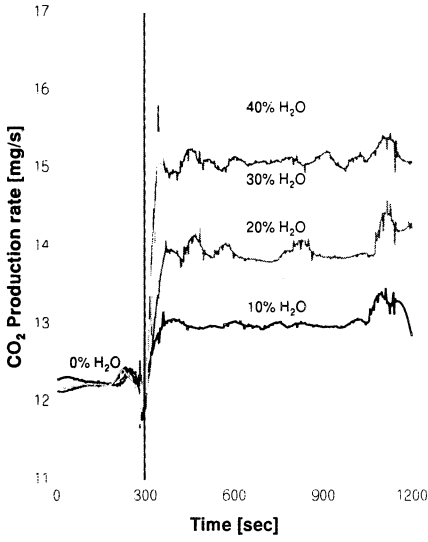


**Fig. 4a:** Measured CO<sub>2</sub> Production rate.

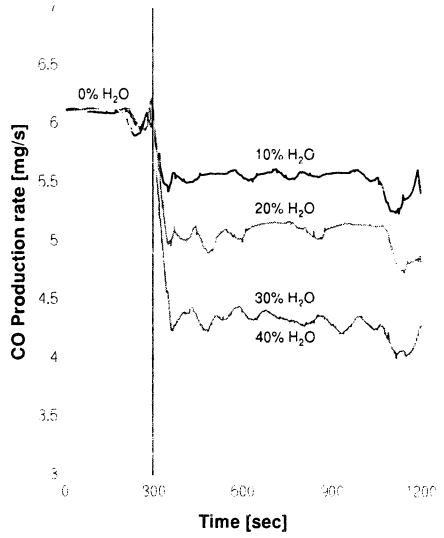


**Fig. 4b:** Measured CO Production Rate

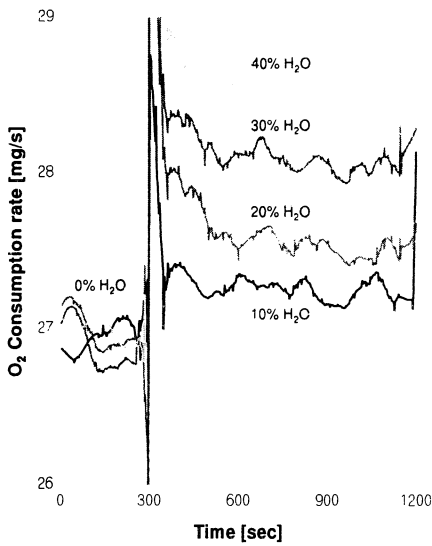


**Fig. 4c:** Measured O<sub>2</sub> Consumption Rate.

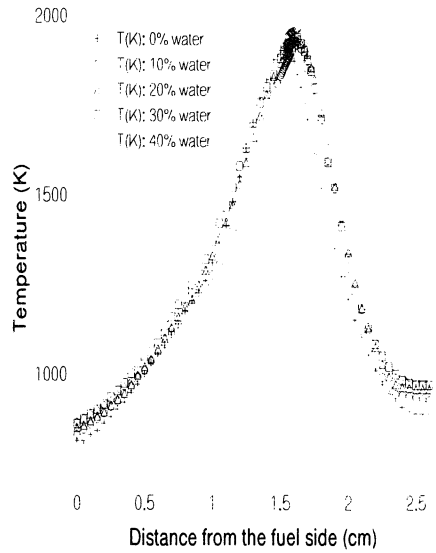


**Fig. 4d:** Measured Flame Temp. Profiles.

**FIGURE 4:** Species production rates for methane flames with H<sub>2</sub>O+Ar mixture replacing N<sub>2</sub> in the oxidizer flow with 20% O<sub>2</sub>. Water vapor +Ar mixture replaced N<sub>2</sub> after 300 seconds.



temperature profiles were also measured along the centerline and normal to the flame by a  $\text{SiO}_2$ -coated  $\text{Pt}/\text{Pt}-\text{Rh}$  thermocouple. The measured temperatures were corrected for radiation for use in numerical calculations.

The mass production rates of  $\text{CO}_2$ ,  $\text{O}_2$  and  $\text{CO}$  for the water flames are shown in figures 4a-4c. Clearly,  $\text{CO}_2$  production is increased,  $\text{CO}$  production is decreased and  $\text{O}_2$  consumption is increased with increasing water concentrations. Visibly, the flames also become less sooty with no net change in the fuel consumption rate. Thus, combustion efficiency is actually increased with an increase in the water vapor concentration and  $\text{CO}$  and possibly soot precursors are being oxidized to  $\text{CO}_2$  as the water concentration is increased. Similar trends were found for 15 & 25%  $\text{O}_2$ . This indicates that the  $\text{CO}$  increase observed in figure 3b was probably due to disruptions caused by water evaporation.

The additional heat released due to oxidation of  $\text{CO}$  and soot precursors to  $\text{CO}_2$  eventually manifests itself in an increase in the flame temperature. Measured temperature profiles for different water vapor substitutions are shown in figure 4d. The temperature profiles have the same shape except the peak temperature and the width is increased. The maximum temperature of the flames was increased slightly with increasing water vapor substitution (1914K for 0% to 1960K for 40% water vapor). There is also a small shift in the location of the peak temperature for the 0% water case. This may be due to change in the transport properties with water vapor substitution.

To summarize, these experiments clearly show that a significant chemical enhancement of combustion is caused by the water used in fire suppression. The actual magnitude of the enhancement depends on the water concentration, the  $\text{O}_2$  concentration and the flame temperatures. Also, mixing caused by liquid water application and water evaporation can significantly affect the gas composition. In particular, an increase in the  $\text{CO}$  concentration in a low  $\text{O}_2$ % fire environment is very disturbing.

## NUMERICAL CALCULATIONS

Numerical calculations with detailed chemistry (GRIMECH-2.11) were done to investigate the flame structure and the effect of flame radiation and strain rate. The Sandia Chemkin-based OPPDIF flame code [17] was modified to include flame radiation. Gas radiation from  $\text{CH}_4$ ,  $\text{O}_2$ ,  $\text{N}_2$ ,  $\text{CO}$ ,  $\text{CO}_2$  and  $\text{H}_2\text{O}$  species was used in the radiative calculations and radiation from soot and other heavy hydrocarbon was not included due to the lack of knowledge of their concentrations. Figure 5a shows the calculated and measured temperatures using the energy equation both with and without gas radiation for the 40% water vapor substitution case (i.e. case (5) of Table 1). The good agreement of the radiative calculation with the experiment concurs with the visual observation that the flame for the 40% water substitution case was significantly less sooty. Thus, ignoring the radiation from soot and other hydrocarbons did not significantly affect the calculated results. Consequently, several calculations were done for the 40% water substitution case with different strain rates (that are likely to be present in a fire during suppression) and with and without flame radiative heat loss.

Figure 5b shows the calculated adiabatic flame temperature profiles at various strain rates for the 40% water vapor substitution case, whereas, fig. 5c shows the corresponding temperature profiles with flame radiation. In these figures, the lowest strain rate corresponds to the

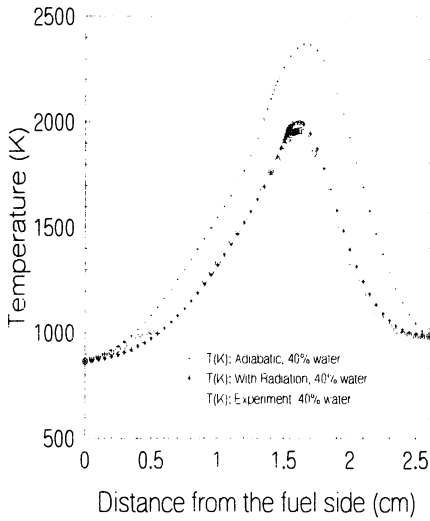


**Fig. 5a:** Calculated and measured temperature profiles for the 40% H<sub>2</sub>O vapor substitution case.

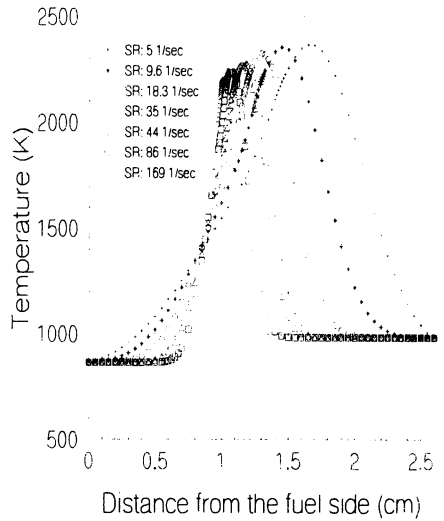


**Fig. 5b:** Calculated adiabatic temperature profiles for different strain rates with 40% water substitution.

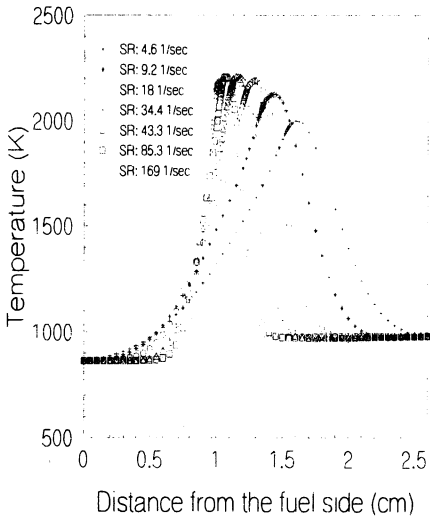


**Fig. 5c:** Calculated temperature profiles for different strain rates with 40% water & radiation.

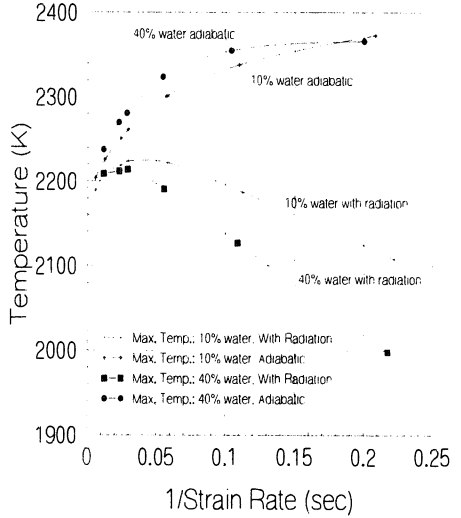


**Fig. 5d:** Variation of the maximum flame temperature with strain rate.

**FIGURE 5:** Numerical Calculations with water for different strain rates with and without flame radiation.

experimental case shown in fig. 5a. As the strain rate is increased, the temperature profile becomes narrower and the location of the maximum temperature moves toward the stagnation plane. For the adiabatic calculations, the maximum temperature drops gradually as the strain rate is increased, whereas, for the radiation compensated calculations, the maximum temperature is increased up to a point and then decreased. As indicated by the temperature profile, the flame is wider in the low strain rate field. Thus, gas radiation becomes an important factor in reducing the peak flame temperature at low strain rates. This effect is reduced when the strain rate is increased because a thin flame sheet can not emit much gas radiation. Figure 5d shows the maximum flame temperature variation due to an increase in the strain rate. At high strain rates, the maximum flame temperatures for adiabatic and radiation compensated calculations are close together, while at low strain rate they are far apart for reasons discussed above. From figure 5d it can also be seen that the maximum flame temperatures for the adiabatic cases (10% and 40%) are not very different. However, for radiation compensated cases, the 40% water substitution case has more radiation effect than the 10% water substitution case. Therefore, as expected, an increase in the water vapor concentration enhances the flame radiation which is more pronounced at lower strain rates.

## CONCLUSIONS

Experimental results indicate that water has a very unique effect on flame chemistry. Water increases the production rate of  $CO_2$  and decreases the  $CO$  production rate and the soot formation rate. As a result, the combustion becomes more complete and the flame temperature is increased as the water concentration is increased. However, the actual magnitude of the chemical enhancement depends on the water concentration, the  $O_2$  concentration and the flame temperatures. Further, mixing caused by liquid water application and water evaporation can significantly affect the gas composition. In particular, it may increase the  $CO$  concentration for a low  $O_2$  concentration fire environment.

Computations of flame temperatures for various strain rates with and without flame radiation show that: (i) The radiation compensated temperatures are closer to the experimental results for high water concentration cases. This is due to an increase in the radiation from water and a simultaneous reduction in the radiation from soot which was not included in the calculations. (ii) For the high strain rate cases, the flame radiation effect is not as significant as for the low strain rate cases due to a reduction in the flame thickness. (iii) As expected, an increase in the water vapor concentration enhances the flame radiation particularly for low strain flames

## ACKNOWLEDGMENTS

Financial support for this work was provided by NIST under the contract number 60NANB5D0109. Suggestions and encouragement during the course of this work from Dr. David D. Evans are also gratefully acknowledged.

## REFERENCES

1. Rasbash, D. J., "The Extinction of Fire with Plain Water: A Review," First International Symposium on Fire Safety Science, 1145-1163, 1986.
2. Heakestad, G., "Role of Water in Suppression of Fire: A Review," Fire and Flammability.

- 2: 254-259, 1980.
3. Evans, D. D., "Overview of Fire Suppression with Water." Proceedings of the Eastern States Section of the Combustion Institute, December, 1988.
  4. Tamanini, F., "Application of Water Sprays to Extinguishment of Crib Fires," Combustion Science and Technology, 14: 1-13, 1976.
  5. Evans, D.D., "Combustion of Wood charcoal," Ph.D. Thesis Harvard University, 1975.
  6. Magee, R. S. and Reitz, R. D., "Extinguishment of Radiation Augmented Plastic Fires by Water Spray," 15th Symposium (International) on Combustion, 337-347, 1975.
  7. Mawhinney, J. R., Dlugogorski, B. Z., Kim, A. K., "A Closer Look at the Fire Extinguishing Properties of Water Mist," Fourth International Symposium on Fire Safety Science, 47-60, 1994.
  8. Abu-Zaid, M., and Atreya, A., "Transient Cooling of Hot Porous and Non-Porous Ceramic Solids by Droplet Evaporation," ASME J. Heat Transfer, 116: 694-701, 1994.
  9. diMarzo, M.; Liao, Y.; Tartarini, P.; Evans, D. D.; Baum, H. R.; "Dropwise Evaporative Cooling of a Low Thermal Conductivity Solid," 3<sup>rd</sup> International Symposium on Fire Safety Science, 987-996, 1991.
  10. Muller-Dethlefs, K., Schlader, A. F., "The Effect of Steam on Flame Temperature Burning Velocity and Carbon Formation in Hydrocarbon Flames," Combustion and Flame, 27: 205-215, 1976.
  11. Koroll, G. W., Mulpuru, S. R., "The Effect of Dilution with Steam on the Burning Velocity and Structure of Premixed Hydrocarbon Flames," Twenty-First Symposium (International) on Combustion, The Combustion Institute, 1811-1819, 1986.
  12. Zhang, C., Atreya, A., Lee, K., "Sooting Structure of Methane Counterflow Diffusion Flames with Preheated Reactants and Dilution by Products of Combustion," Twenty-Fourth Symposium (International) on Combustion, The Combustion Institute, 1049-1057, 1992.
  13. Chung, K.P., Manheimer-Timnat, Y., Yaccarino, P., Glassman, I., "Sooting Behavior of Gaseous Hydrocarbon Diffusion Flames and the Influence of Additives," Combustion Science and Technology, 22: 235-250, 1980.
  14. Seshadri, K., "Structure and Extinction of Laminar Diffusion Flames above Condensed Fuels with Water and Nitrogen," Combustion and Flame, 33: 197-215, 1978.
  15. Crompton, T., "The Physical and Chemical Effects of Water in Laminar Hydrocarbon Diffusion Flames." M.S. Thesis, University of Michigan, Ann Arbor, MI. pp. 9-41, 1995.
  16. Atreya, A., "Pyrolysis, Ignition and Flame Spread on Horizontal Surfaces of Wood," Ph.D. Thesis Harvard University, 1983.
  17. Kee, R. J., Miller, J. A., "A Structured Approach to the Computational Modeling of Chemical Kinetics and Molecular Transport in Flowing Systems," Sandia National Laboratories Report, SAND86-8841, Livermore, CA, 1992.